MSC 57M99 DOI: 10.14529/mmp220301

SYSTEM ANALYSIS OF CLASSIFICATION OF PRIME KNOTS AND LINKS IN THICKENED SURFACES OF GENUS 1 AND 2

A.A. Akimova, South Ural State University, Chelyabinsk, Russian Federation, akimovaaa@susu.ru

In this paper, we present a system analysis of approaches to classification of prime knots and links in thickened surfaces of genus 1 and 2 obtained by the author in collaboration with S.V. Matveev and V.V. Tarkaev in 2012 – 2020. The algorithm of the classification forms structure of the present paper. The results of classification are considered within system analysis of the main ideas of key steps of the algorithm. First, we construct prime projections. To this end, we define a prime link projection, enumerate graphs of special type which embedding in the surface can be a prime projection, enumerate projections in the surface, and show that all obtained projections are prime and not equivalent using some invariants of projections. Second, we construct prime links. To this end, we define a prime link, construct a preliminary set of diagrams, use invariants of links to form equivalence classes of the obtained diagrams and show that the resulting diagrams are not equivalent, and prove primality of the obtained links. At that, at each step, the used methods and the introduced objects are characterized from viewpoints of two cases (genus 1 and 2), and we distinguish properties that are common for both cases or characteristics of only one of two cases. Note consolidated tables, which systematize the classified projections with respect to their properties: generative graph, genus, number of components and crossings, existence and absence of bigon that simplifies the further work with the proposed classification of projections and links.

Keywords: prime projection; knot; link; thickened torus; thickened surface of genus 2; generalised Kauffman bracket polynomial; Kauffman bracket frame; tabulation; classification.

Dedicated to anniversary of Professor A.L. Shestakov

Introduction

In the knot theory, one of the oldest and the most important problems is to recognize a knot (or a link), i. e., to associate the considered object with a unique tabulated one. This problem involves the problem on complete classification of knots and links ordered taking into account some their properties. Most of the classifications obtained during last 150 years consider knots and links in the 3-dimensional sphere S^3, see [1–3]. Recently, increasing interest in the theory of knots and links in arbitrary 3-manifolds (i. e., global knots and links) leads to tabulation of knots and links in manifolds different from the S^3.

As regards tabulation of global knots, note that knots in the solid torus [4] and the thickened Klein bottle [5], as well as prime knots in the lens spaces [6] are tabulated. For the latter, we mention that recent classifications consider only the so-called prime objects, which can not be obtained by some known operations from already tabulated objects. The works [7, 8] present classifications of virtual knots ordered taking into account the number of classical crossings and obtain a list of some characteristics of each knot, but do not take into account such important properties of a knot as primality and genus. Recall that genus of a virtual knot is the minimal genus of the thickened surface which can contain the considered knot. We propose to tabulate virtual knots taking into account both the primality and genus of a knot, see the articles [9, 10] for classifications of prime knots in the thickened surface of genus 1 and 2, respectively, where, in a sense, such classifications are considered as classifications of prime virtual knots of genus 1 and 2.

As regards tabulation of global links, note classifications of links in the projective space [11] and the solid torus [12], as well as prime links in the thickened surface of genus 1 [13, 14] and 2 [15]. Also, we mention a classification of virtual links of special type, namely, alternating virtual links [16], see also [17] for the associated database, which include alternating virtual knots as well.

In this paper, we present a system analysis of approaches to classification of prime knots and links in thickened surfaces of genus 1 and 2 obtained by the author in collaboration with S.V. Matveev and V.V. Tarkaev in 2012 – 2020. After Section 1 that gives main objects considered in this paper, we present the algorithm of the classification that forms structure of the present paper as follows. In Section 2, we construct prime projections. First, in Subsection 2.1, we define a prime link projection. Second, in Subsection 2.2, we enumerate graphs of special type which embedding in the surface can be a prime projection. Third, in Subsection 2.3, we enumerate prime projections in the surface. For this purpose, it is sufficient to enumerate all possible embeddings of the graphs into the surface giving prime link projections. Finally, in Subsection 2.4, we show that all obtained projections are not equivalent in the sense of homeomorphism of the surface onto itself. To this end, we use some invariants of projections. Next, we use the obtained table of prime projections to construct prime links in Section 3. First, in Subsection 3.1, we define a prime link. Second, in Subsection 3.2, we construct a preliminary set of diagrams. To this end, we associate each tabulated projection with the corresponding set of diagrams. Third, in Subsection 3.3, we use invariants of links in order to form equivalence classes of the obtained diagrams and show that all obtained diagrams are not equivalent in the sense of homeomorphism of the surface onto itself. Finally, in Subsection 3.4, we prove primality of the obtained links. Therefore, we describe main ideas of each step of the algorithm and illustrate these steps by results obtained by us within classification of prime knots and links in thickened surfaces.

1. Definitions

In this section, we recall some main objects considered in this paper.

Let T_g be a 2-dimensional surface of genus $g \in \{1, 2\}$ (in the case of $g = 1$, the surface is said to be a torus). Further, for shortness, we omit the words "2-dimensional" and define T_g, $g \in \{1, 2\}$, in more details.

A torus $T_1 = S^1 \times S^1$ can be considered as a direct product of two copies of an 1-dimensional sphere S^1, which are said to be meridian and longitude of T_1 (within the paper, see Fig. 1(a)).

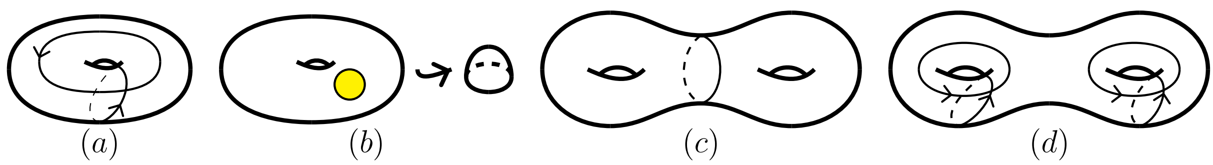

Fig. 1. (a) T_1 endowed with an oriented pair "meridian-longitude", (b) T_1^o with a hole and a disk D^2, (c) T_2 obtained as a result of gluing two copies of T_1^o, (d) T_2 endowed with oriented pairs "meridian-longitude" of its handles

A surface F^o with a hole is obtained from the original surface F by removing the interior of a 2-dimensional disk D^2. Fig. 1(b) shows an example: a torus T_1^o with a hole is obtained from a torus T_1 by removing the interior of a disk D^2. Hereinafter, we use ^{o} to show that a surface has one hole and ^{oo} to show that a surface has two holes.

In its turn, T_2 can be considered as a surface formed by gluing two copies of a torus T_1^o with a hole constructed by identifying their holes, see Fig. 1(c). Here each T_1^o is called a handle of T_2. In other words, T_2 is a connected sum of two copies of T_1. Note that T_2 also admit consideration of a fixed pair "meridian-longitude" for each of its handles (within the paper, see Fig. 1(d)).

Consider a surface T_g, where $g \in \{1, 2\}$, and an interval $I = [0, 1]$. A thickened surface of genus g is a 3-dimensional manifold homeomorphic to the direct product $T_g \times I$.

Denote by $L_m \subset T_g \times I$ an m-component link in $T_g \times I$, which is defined as a smooth embedding of m simple closed curves, union of which forms a not connected 1-dimensional manifold, in the interior of $T_g \times I$ such that the images of the curves do not intersect each other. Note that 1-component link L_1 is said to be a knot and is denoted by K. Two links $L_m \subset T_g \times I$ and $L'_m \subset T_g \times I$ are said to be equivalent, if there exists a homeomorphism of $T_g \times I$ onto itself that takes L_m to L'_m.

As in the classical case, links in $T_g \times I$ can be presented by their diagrams. A diagram $D \subset T_g$ of a link $L_m \subset T_g \times I$ is defined by analogy with a diagram of a classical link except that the link is projected into the surface T_g instead of the plane. For each component of L_m, we refer to the part of D associated with this component as the component of D. Two diagrams D and D' in T_g are equivalent, if there exists a sequence of Reidemeister moves $\Omega_1 - \Omega_3$ and simultaneous switchings of types of all crossings that takes D to D'.

A projection $G \subset T_g$ of a link $L_m \subset T_g \times I$ is a diagram of L_m such that the crossings of the diagram are transversal intersections of strands without any under/over-crossing information. Therefore, a projection is a subset of T_g such that each connected component of the subset is a regular graph of degree 4 embedded in T_g. Two projections G and G' in T_g are equivalent, if there exists a homeomorphism of T_g onto itself that takes G to G'. For the given projection $G \subset T_g$, we consider the following characteristics: crossings are vertices of G, complexity is the number of crossings, faces are connected components of the set $T_g \setminus G$, components are closed paths on G passing through crossings of G by the "straight ahead" rule. It is clear that if G is obtained by projection of a link L_m into T_g, then each component of G is a projection of the corresponding component of L_m.

Within the presented below classification, we fix a genus $g \in \{1, 2\}$ of the surface, a number $n \in \{2, ..., 5\}$ of crossings in a diagram and a number $m \in \{1, 2, ..., 4\}$ of components of a link (we use $m = 1$ in the case of a knot and below refer to a knot as an 1-component link).

2. Construction of Prime Projections

First, in Subsection 2.1, we define a prime link projection. Second, in Subsection 2.2, we enumerate graphs of special type which embedding in the surface can be a prime projection. Third, in Subsection 2.3, we enumerate prime projections in the surface. Finally, in Subsection 2.4, we show that all obtained projections are not equivalent in the sense of homeomorphism of the surface onto itself.

2.1. Definition of Prime Projection

In the knot theory, recent classifications consider only the so-called prime objects, which can not be obtained by some known operations from already tabulated objects. Therefore, in this subsection, we define a prime link projection in T_g. First of all, Table 1 compares types of simple closed curves considered in T_1 and T_2, see also Fig. 1(b,c) and Fig. 1(a,d) for examples of cut and not cut curves, respectively. Then, Table 2 presents comparison of types of link projections in T_1 and T_2 necessary to define a prime projection. Lemma 1 establishes a connection between types of links given in Subsection 3.1 (see Table 5) and types of projections defined in Table 2.

Table 1

Types of a simple closed curve $C \in T_g$, $g \in \{1,2\}$

<table>
<tr><td>Type</td><td>$C, C' \in T_1$, see [14]</td><td>$C, C' \in T_2$, see [18]</td></tr>
<tr><td>Cut</td><td colspan="2">The complement $T_g \backslash C$ consists of two components.</td></tr>
<tr><td>Trivial cut</td><td colspan="2">$T_g \backslash C = T_g^o \cup D^2$</td></tr>
<tr><td>Not trivial cut</td><td>–</td><td>$T_2 \backslash C = T_1^o \cup T_1^o$</td></tr>
<tr><td>Not cut</td><td colspan="2">The complement $T_g \backslash C$ consists of the unique component: T_{g-1}^{oo}, where T_0^{oo} is considered as a 2-dimensional sphere with 2 holes.</td></tr>
<tr><td>Parallel not cut</td><td colspan="2">$T_g \backslash \{C \cup C'\} = T_{g-1}^{oo} \cup T_0^{oo}$</td></tr>
</table>

Table 2

Types of a link projection $G \in T_g$, $g \in \{1,2\}$

<table>
<tr><td>Type</td><td>$G \in T_1$, see [14]</td><td>$G \in T_2$, see [18]</td></tr>
<tr><td>Essential</td><td colspan="2">Each face of G is homeomorphic to D^2.</td></tr>
<tr><td rowspan="4">Composite</td><td colspan="2">At least one of the following conditions holds.</td></tr>
<tr><td colspan="2">(a) There exists a disk $D^2 \subset T_1$ such that the boundary ∂D^2 intersects G transversally exactly in two points, which are internal for two distinct edges of G, and at least one vertex of G is inside D^2.</td></tr>
<tr><td colspan="2">(b) There exist two not cut parallel simple closed curves $C_1, C_2 \subset T_g$ and two distinct edges e_1, e_2 of G such that for $i = 1, 2$ the curve C_i intersects the edge e_i transversely at exactly one internal point, and both surfaces (T_{g-1}^{oo} and T_0^{oo}) to which the curves divide T_g contain vertices of G.</td></tr>
<tr><td>–</td><td>(c) There exists a not trivial cut simple closed curve $C \subset T_2$ and two distinct edges e_1, e_2 of G such that C intersects the edge e_i, $i = 1, 2$, transversely at exactly one internal point, and both surfaces (two copies of T_1^o) to which the curve C divide T_2 contain vertices of G.</td></tr>
<tr><td>Split</td><td colspan="2">There exists a component of G that has no common points or exactly one common point with the union of all other components of G.</td></tr>
<tr><td>Prime</td><td colspan="2">G is essential, not composite and not split.</td></tr>
</table>

Lemma 1. [14, Lemma 2.1] *Let L be a link in $T_g \times I$ having diagram $D \subset T_g$ on the projection $G \subset T$. If the projection G is composite, split or essential, then the link L is composite, split or essential, respectively.*

2.2. Enumeration of Graphs

Let us enumerate graphs whose embedding into T_g can be a prime projection.

Lemma 2. [14, Lemma 4.2] *If a projection $G \subset T$ is prime, then G is connected and contains no loop nor any cut pair of edges (i.e., removing the pair of edges gives a disconnected graph).*

All abstract quadrivalent graphs with at most 5 vertices satisfying the first and second conditions were enumerated in [9]. In this list, there are exactly 8 graphs satisfying the third condition of Lemma 2, see graphs $a - h$ given in Fig. 2.

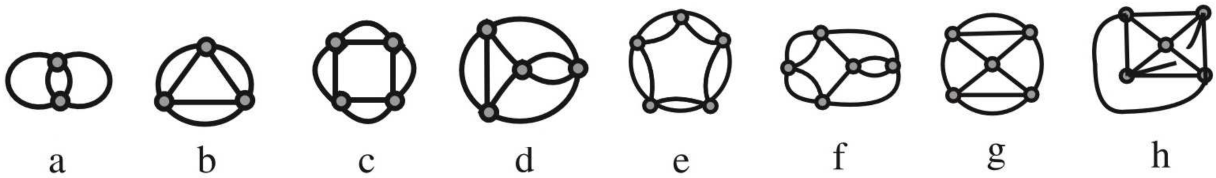

Fig. 2. Graphs used to enumerate prime projections

2.3. Enumeration of Prime Projections

We use the graphs obtained in Subsection 2.2 to construct prime projections by representing an embedding of each graph as an union of curves and enumerating all possible combinations of types of intersection points (transversal or not transversal (see [18])), and curves (cut (for T_2, trivial or not trivial) or not cut (for T_2, parallel or not)).

A face of a projection is called bigon, if the face is homeomorphic to D^2 and the boundary of the face is composed of exactly two edges. The transformation of a projection that creates or removes a bigon (see Fig. 3 on the left) turned out to be useful to construct most part of projections in T_1 (i.e., all projections with at least one bigon). In this case, we reduce consideration of a graph with n vertices to a graph with $n-2$ vertices, which does not necessary satisfy conditions of Lemma 2 and even can be a circle without vertices. For the rest (without bigons) projections in T_1 and all projections in T_2, we use transformation of a projection that add or remove a nontransversal point (see Fig. 3 on the right).

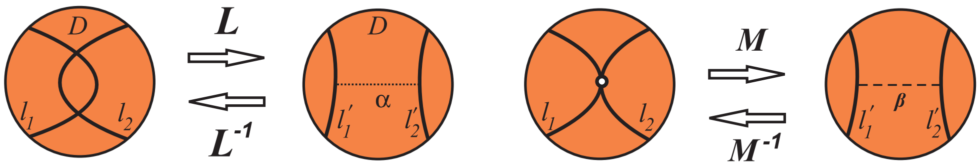

Fig. 3. L removes a bigon, while L^{-1} is performed along the dotted arc α and creates a bigon; M removes a nontransversal point, while M^{-1} is performed along the dashed arc β and creates a nontransversal point

Table 3 presents integrated data on numerical results of embedding of the graphs $a-h$ given in Fig. 2 that leads to prime projections in T_g, $g \in \{1, 2\}$, which were obtained in [9, 13, 14, 18, 19]. Table 4 presents integrated data on numerical results of tabulation of prime projections and diagrams in T_g, $g \in \{1, 2\}$, which were obtained in [9, 10, 13–15, 18, 19].

2.4. Invariants of Projections

In order to show that all obtained projections are not equivalent in the sense of homeomorphism of the surface onto itself, we use some invariants of projections [13, 18, 19].

The first invariant, which turned out to be enough to prove that the most part of projections are pairwise inequivalent, is constructed as follows. First, we associate each face of a projection with a natural number, which is equivalent to the number of edges which form the boundary of the face. Since each face of a prime projection is homeomorphic to D^2, then the number of faces of each projection is equal to $n-2g+2$, where n is the number of crossings and g is the genus of the surface T_g. Second, we associate each projection with an ordered set $\{[g]\ (m)\ i_1\ i_2\ \ldots\ i_{n-2g+2}\ x\}$, where g is the genus of the surface T_g, m is the number of components of the projection, $1 \le m \le 4$, $i_1,\ i_2,\ \ldots,\ i_{n-2g+2}$ are natural numbers, which are associated with faces of the projection and put in not decreasing order, n is the number of crossings, x is the graph such that the projection is an embedding of x in T_g, $x \in \{a,b,c,d,e,f,g,h\}$, see Fig. 2.

Table 3

Prime projections obtained as embedding of the graphs $a-h$ in T_g [9,13,14,18,19]

Graph	Genus	Number of components	Prime projections with bigons	Prime projections without bigons
a	1	1	2_1 [9]	–
		2	–	2_1 [13]
b	1	1	3_1, 3_2 [9]	3_1 [9]
		2	3_1 [13]	3_2, 3_3 [13]
		3	–	3_4 [13]
	2	1	–	3_1 [19]
		2	–	3_1 [18]
c	1	1	4_1, 4_3, 4_8 [9]	[9]
		2	4_1, 4_3, 4_6 [13]	4_9 [13]
		4	–	4_{13} [13]
	2	1	4_1 [19]	4_6 [19]
		2	–	4_4 [18]
		3	–	4_{11} [18]
		4	–	4_{14} [18]
d	1	1	4_2, 4_4-4_7, 4_9 [9]	4_{10} [9]
		2	4_2, 4_4, 4_5, 4_7 [13]	–
		3	4_8 [13]	4_{10}-4_{12} [13]
	2	1	4_2, 4_3 [19]	4_4, 4_5, 4_7-4_{13} [19]
		2	4_1, 4_2 [18]	4_3, 4_5- 4_9 [18]
		3	4_{10} [18]	4_{12}, 4_{13} [18]
		4	–	4_{14} [18]
e	1	1	5_1, 5_2, 5_4, 5_6, 5_{31} [9]	–
		2	5_1, 5_{10}, 5_{13}, 5_{16} [13]	5_{36} [13]
f	1	1	5_3, 5_5, 5_7, 5_{10}, 5_{12}, 5_{14}, 5_{16}-5_{18}, 5_{22}, 5_{27}, 5_{28}, 5_{32} [9]	–
		2	5_2, 5_3, 5_5, 5_8, 5_{11}, 5_{14}, 5_{18}, 5_{21} [13]	5_{34} [13]
		3	5_{38}, 5_{40}-5_{43} [13]	[13]
		4	–	5_{47} [13]
g	1	1	5_8, 5_9, 5_{11}, 5_{13}, 5_{15}, 5_{19}-5_{21}, 5_{23}-5_{26}, 5_{29}, 5_{30} [9]	5_{34} [9]
		2	5_4, 5_6, 5_7, 5_9, 5_{12}, 5_{15}, 5_{17}, 5_{19}, 5_{20}, 5_{22}-5_{30} [13]	5_{32} [13]
		3	5_{39} [13]	5_{45} [13]
		4	–	5_{46} [13]
h	1	1	–	5_{33} [9]
		2	–	5_{31}, 5_{33}, 5_{35}, 5_{37} [13]
		3	–	5_{44} [13]

Table 4

Prime projections and diagrams of the type $(g;m;n)$ obtained in [9,10,13–15,18,19]

Genus, $g \in \{1,2\}$	Components, $m \in \{1,2,3,4\}$	Crossings, $n \in \{2,3,4,5\}$	Prime projections of the type $(g;m;n)$	Prime diagrams of the type $(g;m;n)$
1	1	2	2_1 [9]	2_1 [9]
		3	3_1, 3_2 [9]	3_1-3_3 [9]
		4	4_1-4_{10} [9]	4_1-4_{17} [9]
		5	5_1-5_{34} [9]	5_1-5_{69} [9]
	2	2	2_1 [13]	2_1 [14]
		3	3_1-3_3 [13]	3_1-3_3 [14]
		4	4_1-4_9 [13]	4_1-4_{17} [14]
		5	5_1-5_{37} [14]	5_1-5_{79} [14]
	3	3	3_4 [13]	3_4 [14]
		4	4_{10}-4_{12} [13]	4_{18}-4_{20} [14]
		5	5_{38}-5_{45} [14]	5_{80}-5_{97} [14]
	4	4	4_{13} [13]	4_{21} [14]
		5	5_{46}, 5_{47} [14]	5_{98}, 5_{99} [14]
2	1	3	3_1 [19]	3_1-3_3 [10]
		4	4_1-4_{13} [19]	4_1-4_{72} [10]
	2	3	3_1 [18]	3_1 [15]
		4	4_1-4_9 [18]	4_1-4_{31} [15]
	3	4	4_{10}-4_{13} [18]	4_{32}-4_{36} [15]
	4	4	4_{14} [18]	4_{37} [15]

In order to define the second invariant, we say that an edge e of the projection G has type (i,j) if e is a common edge of i-gonal and j-gonal faces of the projection G. The existence and absence of edges of some type allow to prove pairwise inequality of some projections in T_g, $g \in \{1,2\}$.

Third, for some pairs of projections in T_1, we use the existence and absence of common points of i-gonal and j-gonal faces, e.g. if each of the three triangle faces of G_1 has a common point with its bigon while G_2 has a triangle face having no common points with its bigon, then G_1 and G_2 are pairwise inequivalent.

Fourth, for some pairs of projections in T_2, we recall that the “straight ahead” rule determines a cycle composed of all edges of the projection, and think about different number of edges of the type (i_1,j_1) between edges of the type (i_2,j_2) in such a cycle.

The fifth invariant is used for projections in T_2 and takes into account absence of bijective mapping between Gauss codes of the projections, i.e. sequences of ordinal numbers of vertices taking in the order of visiting the vertices then go along the projection by “straight ahead” rule.

The sixth invariant is used for projections in T_2 and takes into account absence of self intersections of a component.

Finally, for some pairs of projections in T_2, we use the existence and absence of an edge, which is common for the same face, or the number of edges that are common for different faces with the same number of vertices.

3. Construction of Prime Links

In this section, we tabulate prime not oriented links in the thickened surface $T_g \times I$, $g \in \{1,2\}$. Namely, we construct a table of prime diagrams based on the table of prime link projections obtained in Section 2 as follows. First, in Subsection 3.1, we define a prime link. Second, in Subsection 3.2, we construct a preliminary set of diagrams. To this end, we associate each tabulated projection with the corresponding set of diagrams. Third, in Subsection 3.3, we use invariants of links in order to form equivalence classes of the obtained diagrams and show that all obtained diagrams are not equivalent. Finally, in Subsection 3.4, we prove primality of the obtained links.

3.1. Definition of Prime Link

First of all, we recall definition of destabilization. Assume that $D \subset T_g$ is a link diagram. A not cut curve $C \subset T_g$ is said to be a cancellation curve for the pair (D, T_g), if an intersection of C and D is empty. In order to perform destabilization of the surface T_g, it is sufficient to cut T_g along the cancellation curve C and glue each obtained component of the boundary by a disk D^2. Fig. 4 shows a torus T_1 as a result of destabilization of T_2.

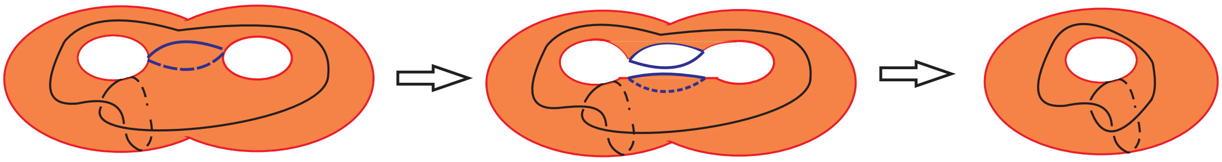

Fig. 4. Destabilization of T_2

Table 5 presents comparison of types of links in T_1 and T_2.

Table 5

Types of a link $L \in T_g,\ \ g \in \{1, 2\}$

Type	$L \in T_1$, see [14]	$L \in T_2$, see [15]
Essential	Any diagram of L admits no destabilization, i.e. any annulus, which is isotopic to $C \times I \subset T_g \times I$, where $C \subset T_g$ is a not cut simple closed curve, has not empty intersection with L.	
Composite	At least one of the following conditions holds.	
	(a) L is a connected sum of essential links $L' \subset T_g \times I$ and $L'' \subset S^3$ defined by analogy with the classical connected sum of two links in S^3, see [10, 13, 15] for more details.	
	(b) L is a circular connected sum of two essential links $L' \subset T_g \times I$ and $L'' \subset T_1 \times I$ introduced in [20] and generalised for T_2 in [10, 15].	
	–	(c) L is a connected sum of two essential links L, L' in $T_1 \times I$ introduced in [10, 15].
Split	There exists an embedded surface in $T_g \times I$ (i.e., T_g, T_{g-1}, T_{g-2} (if any)), which does not intersect L and cuts $T_g \times I$ into two parts such that each part contains a component of L.	
Prime	L is essential, not composite and not split.	

The natural idea is to tabulate only prime links. Indeed, nonessential links correspond to links that can be found in already existing tables of knots and links in the 3-dimensional sphere S^3 [1–3] or thickened annulus (solid torus) [4, 12]. In their turn, composite links correspond to links, which can be obtained using already known knots and links by connected sums of the types $(a) - (c)$. Finally, a split link can be considered as a trivial union of already tabulated knots and links.

3.2. Construction of Preliminary Set of Diagrams

We convert each prime link projection constructed in Section 2 to the set of corresponding diagrams. To this end, we enumerate all possible ways to consider each crossing of a projection to be either an over- or undercrossing of a diagram. Obviously, there are 2^n diagrams on each projection with n crossings. However, we can significantly reduce this procedure by the following three ideas [14].

First, the simultaneous switching of all crossings convert any diagram to the equivalent one. Therefore, we can fix the type of one crossing of each projection and, consequently, to halve the set of diagrams on the projection.

Second, if a diagram is based on a projection having biangle face, then both crossings of the face have the same type. Otherwise, we can reduce the number of crossings by the second Reidemeister move Ω_2, see also [9] for detailed information of alternate fragments of projections that allow to simplify enumeration of possibilities.

Third, each component of a diagram contains both types of crossings (under- and over-crossings) with the union of other components, otherwise we have a split diagram, since there exists the necessary embedded T_g.

3.3. Invariants of Links

In order to form equivalence classes of the obtained diagrams, we use invariants of nonoriented links, which are based on the Kauffman bracket [21] (see also [22] for the original version called the Jones polynomial).

3.3.1. Generalized Kauffman Bracket Polynomial for T_1

Let us recall the definition of the generalized Kauffman bracket polynomial [13]. In contrast to the usual Kauffman bracket polynomial of classical knots [21], the generalized version takes into account types of curves on the surface (cut and not cut).

Let D be a diagram of a knot or link on T_1. Endow each angle of each crossing of D with a marker A or B according to the rule given in the center of Fig. 5(a). Each state s of the diagram D is defined by a combination of ways to smooth each crossing of D such as to join together either two angles endowed with a marker A, or two angles endowed with a marker B, see Fig. 5(a) on the left and right, respectively. Obviously, if the diagram D has n crossings, then there exist exactly 2^n states of D.

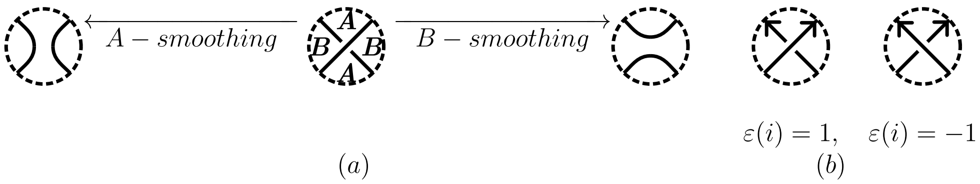

Fig. 5. (a) A- and B-smoothings of a crossing, (b) rules to define the sign $\varepsilon(i)$ of the i-th crossing

By the writhe of an oriented classical knot diagram D with n crossings we mean the sum over all crossings of D

$$w(D) = \sum_{i=1}^{n} \varepsilon(i),$$

where $\varepsilon(i)$ is a sign of the i-th crossing of D defined by the rules given in Fig. 5(b). Note that the writhe of an oriented classical link diagram is the sum of signs of only those crossings of D that are self-intersections of the components.

The exact formula of the generalized Kauffman bracket polynomial [13] is as follows:

$$\mathcal{X}\left(a, x\right)_D = (-a)^{-3w(D)} \left\langle a, x\right\rangle_D , \tag{1}$$

where

$$\left\langle a, x\right\rangle_D = \sum_s a^{\alpha(s)-\beta(s)}(-a^2 - a^{-2})^{\gamma(s)} x^{\delta(s)} \tag{2}$$

is the generalized Kauffman bracket [13]. Here $\alpha(s)$ and $\beta(s)$ are the numbers of markers A and B in the given state s, while $\gamma(s)$, $\delta(s)$ are the numbers of cut and not cut curves in T_1 obtained by smoothing of all crossings according to the state s, and $w(D)$ is the writhe of D. The sum is taken over all 2^n states of D.

3.3.2. Kauffman Bracket Skeleton for T_1

Let us define the Kauffman bracket skeleton [14] as a simplification of the generalized Kauffman bracket polynomial $\mathcal{X}\left(a, x\right)_D$. Obviously, $\mathcal{X}\left(a, x\right)_D$ can be represented in the form

$$\mathcal{X}\left(a, x\right)_D = \sum_m P_m(a) x^m,$$

where $P_m(a) = \sum\limits_j b_{jm} a^j$ is a Laurent polynomial.

Let t_m be a tuple composed of nonzero coefficients b_{jm} of the polynomial $P_m(a)$, which are ordered in increasing order of j. Note that transition from $P_m(a)$ to t_m erases information on degrees of the variable a and remains information on order and values of the coefficients b_{jm}. For example, Laurent polynomials $P_{m_1}(a) = a^{-10} + 5a^{10}$ and $P_{m_2}(a) = 1 + 5a^2$ correspond to the same tuple $t_{m_1} = t_{m_2} = (1, 5)$.

The formal sum

$$S_D = \sum_{t_m \neq \emptyset} t_m x^m \tag{3}$$

is called the Kauffman bracket skeleton, and tuples t_m are called coefficients of the Kauffman bracket skeleton. We say that the Kauffman bracket skeletons S_{D_1} and S_{D_2} are inverted to each other, if the coefficients of S_{D_1} are the corresponding coefficients of S_{D_2}, where numbers of each t_m are taken in reverse order. This transformation of the Kauffman bracket skeletons is called inversion. For example, $S_{D_1} = (1, -2)x + (3, -4, 2)x^3$ is inverted to $S_{D_2} = (-2, 1)x + (2, -4, 3)x^3$.

Lemma 3. [14, Corollary 4.12] *The Kauffman bracket skeleton considered up to inversion and multiplication by* -1 *is an invariant of links in the thickened torus.*

Note that the generalized Kauffman polynomial $\mathcal{X}\left(a, x\right)_D$ is stronger than the Kauffman bracket skeleton $S_{\langle D\rangle}$, while $S_{\langle D\rangle}$ is more compact and has equal strength within the considered problem. Computation of both $\mathcal{X}\left(a, x\right)_D$ and $S_{\langle D\rangle}$ is implemented in the program “3-Manifold Recognizer” [23].

3.3.3. Additional Invariants for T_1

With the exception of some pairs, the list of the generalizations of the Kauffman bracket described above is enough to prove that all tabulated links in T_1 are pairwise inequivalent. For the rest links, we use the following two invariants [14]. First invariant for T_1 takes into account the existence and absence of a homology trivial component. In order to describe the second invariant for T_1, choose and fix any orientation of each link. The orientation allows to consider the homology classes of components of the links and to find the intersection number of these homology classes, which absolute value is an invariant of nonoriented link.

3.3.4. Kauffman Bracket Frame for T_2

Kauffman bracket frame $\mathfrak{F}(\cdot)$ was obtained in [24] as a simplification of the surface bracket polynomial [25]. The idea of the invariant is to consider only the values and order of coefficients and do not take into account the powers of one of the variables.

Define coordinates of not cut curves in T_2 as follows. For any oriented not cut curve $C \subset T_2$ and two fixed oriented pairs "meridian-longitude" of handles of the surface T_2 (within the paper, see Fig. 1(d)), the numbers a and c (respectively, b and d) are calculated as intersection numbers of the curve C and the corresponding meridian (respectively, longitude) of the surface T_2. Then the curve C is associated with the ordered set of four numbers (a, b, c, d), where a, b, c, d are called the coordinates of the curve C. The coordinates (a, b, c, d) and $(-a, -b, -c, -d)$ are considered to be equal.

For the given diagram $D \subset T_2$, we define the set of states as described above for the generalized Kauffman bracket polynomial for T_1. Associate the union of disjoint not cut curves in each state s_i, $i = 1, 2, 3, \ldots, 2^n$, with a product of the corresponding variables y_j, which take values in the coordinates (a_j, b_j, c_j, d_j) of the not cut curves that form the union associated with s_i. Then the formula of the generalised Kauffman bracket is as follows:

$$\langle a, y_j \rangle_D = \sum_{i=1}^{2^n} a^{\alpha(s_i)-\beta(s_i)} (-a^2 - a^{-2})^{\gamma(s_i)} \prod_j y_j^{\delta_j(s_i)}, \tag{4}$$

where $\delta_j(s_i)$ is the number of not cut curves having coordinates (a_j, b_j, c_j, d_j) associated with the variable y_j.

For shortness, we propose to use the following simplification of (4). Let us order terms of (4) in nondecreasing order of the powers of the variable a and collect terms having the same power of the variable a, i.e. represent (4) as $\sum\limits_m P_m a^m$, where P_m is a polynomial in the variables y_j. Then, we associate the polynomial (4) with an ordered set of nonzero polynomials P_m in the variables y_j, which is called the Kauffman bracket frame $\mathfrak{F}(\cdot)$. For example, $\widetilde{\mathcal{X}}(D) = -2a^{-8}y_{12} - a^{-12}y_{62} - a^{-8}y_3y_7 - a^{-6}y_4y_7$ is associated with $\mathfrak{F}(D) = (-y_{62}, -2y_{12} - y_3y_7, -y_4y_7)$.

We say that the Kauffman bracket frames $\mathfrak{F}(D_1)$ and $\mathfrak{F}(D_2)$ are inverted to each other, if the elements of $\mathfrak{F}(D_1)$ are the corresponding elements of $\mathfrak{F}(D_2)$, where the polynomials P_m are taken in reverse order. This transformation of the Kauffman bracket frames is called an inversion. For example, $\mathfrak{F}(D_1) = (-y_{62}, -2y_{12} - y_3y_7, -y_4y_7)$ is inverted to $\mathfrak{F}(D_2) = (-y_4y_7, -2y_{12} - y_3y_7, -y_{62})$.

Lemma 4. [10, Lemma 1] *The Kauffman bracket frame $\mathfrak{F}(\cdot)$ considered up to inversion, multiplication by -1, and changes of variables y_j associated with changes of the corresponding homology classes of noncut curves in the surface T_2 generated by orientation preserving homeomorphisms of T_2 is an invariant of knots in the thickened surface $T_2 \times I$ of genus 2.*

3.3.5. Additional Invariants for T_2

With the exception of some pairs, the list of the Kauffman bracket frames described above is enough to prove that all tabulated links in T_2 are pairwise inequivalent. For the rest links, we use the cabled Jones polynomial, see the invariants of the virtual knots given in [7] and the generalised Alexander polynomials [26].

3.4. Proof of Primality

In order to prove that a link is prime, it is enough to show that the link is essential, not composite and not split.

3.4.1. Links in T_1

Following [14], in order to show that a link $L \subset T_1$ is essential, not split and can not be represented as a connected sum of type (a), it is enough to show that the complement of each tabulated link admits the hyperbolic structure. Here by the complement of link we mean $T_1 \times I \setminus U(L)$, where L is a link and $U(L)$ is an open regular tabular neighbourhood of L. We use the program "SnapPy" [27] to verify that the complement of each tabulated link admits the hyperbolic structure. To this end, we use the program "3-Manifold Recognizer" [23] to find the isometric signatures of complements of the tabulated links necessary to compute the hyperbolic volumes by means of the program "SnapPy". The question about representation of tabulated links in T_1 as a circular connected sum is opened. Therefore, some tabulated links can be not prime, if they are circular connected sums.

3.4.2. Links in T_2

Lemma 5. [15, Lemma 2] *Suppose that the Kauffman bracket frame $\mathfrak{F}(D)$ of a connected link diagram $D \subset T_2$ contains terms corresponding to 4 not cut curves having not equivalent coordinates (a_k, b_k, c_k, d_k), $k \in \{1,2,3,4\}$, such that the system of 4 linear equations of the form*

$$b_k \cdot a - a_k \cdot b + d_k \cdot c - c_k \cdot d = 0, \quad k \in \{1,2,3,4\},$$

where a, b, c, d are the variables and a_k, b_k, c_k, d_k are known coefficients, has only zero solution. Then the link diagram D admits no destabilisation.

Following Lemma 5, for each tabulated diagram D, we construct a set of 4 not cut curves involved in the Kauffman bracket frame $\mathfrak{F}(D)$, which is enough to show that there exists no cancellation curve for the corresponding link $L \subset T_2 \times I$, i.e. the link is essential.

In order to prove that all tabulated links are noncomposite, it is enough to show that each knot can not be represented as a connected sum of the type (a), (b), or (c) under the hypothesis that the complexity of a connected sum is not less than the sum of complexities of the terms that form the sum. Within the considered problem on tabulation of links having diagrams with either 3 or 4 crossings, the impossibility of representation as a connected sum of the type (a), (b), or (c) is obvious, see [10, 15] for more details.

As regards to the split property, we note that when constructing the table, we remove obviously split links.

Acknowledgements. *The author is grateful to Professor G.A. Sviridyuk for the problem statement. The work is supported by the RFBR grant No. 20-01-00127.*

References

1. Hoste J., Thistlethwaite M., Weeks J. The First 1,701,936 Knots. *The Mathematical Intelligencer*, 1998, vol. 20, no. 4, pp. 33–47.
2. Rolfsen D. *Knots and Links.* Berkeley, Publish or Perish, 1976.

3. Bar-Natan D. *The Hoste-Thistlethwaite Link Table.* Available at: http://katlas.org/wiki/Main_Page (accessed on July 25, 2020).
4. Gabrovšek B., Mroczkowski M. Knots in the Solid Torus up to 6 Crossings. *Journal of Knot Theory and Its Ramifications*, 2012, vol. 21, no. 11, article ID: 1250106, 43 p. DOI: 10.1142/S0218216512501064
5. Matveev S.V., Nabeeva L.R. Tabulating Knots in the Thickened Klein Bottle. *Siberian Mathematical Journal*, 2016, vol. 57, issue 3, pp. 542–548. DOI: 10.1134/S0037446616030174
6. Gabrovšek B. Tabulation of Prime Knots in Lens Spaces. *Mediterranean Journal of Mathematics*, 2017, vol. 14, no. 2, article ID: 88, 24 p. DOI: 10.1007/s00009-016-0814-5
7. Green J. *A Table of Virtual Knots.* Available at: http://katlas.math.toronto.edu/wiki/ (accessed on July 25, 2018).
8. Stenlund E. *Classification of Virtual Knots.* Available at: http://evertstenlund.se/knots/Virtual%20Knots.pdf (accessed on July 25, 2020).
9. Akimova A.A., Matveev S.V. Classification of Genus 1 Virtual Knots Having at Most Five Classical Crossings. *Journal of Knot Theory and Its Ramifications*, 2014, vol. 23, no. 6, article ID: 1450031. DOI: 10.1142/S021821651450031X.
10. Akimova A.A. Classification of Prime Knots in the Thickened Surface of Genus 2 Having Diagrams with at Most 4 Crossings. *Journal of Computational and Engineering Mathematics*, 2020, vol. 7, no. 1, pp. 32–46. DOI: 10.14529/jcem200103
11. Drobotukhina Yu.V. Classification of Links in $\mathbb{R}$ P^3 with at Most Six Crossings. *Notes of Scientific Seminars POMI*, 1991, vol. 193, pp. 39–63. (in Russian)
12. Akimova A.A. Mathematical Modelling of Biology Processes Based on the Table of Prime Links in the Solid Torus up to 4 Crossings. *Journal of Physics*, 2021, vol. 1847, article ID: 012025, 12 p. DOI: 10.1088/1742-6596/1847/1/012025
13. Akimova A.A., Matveev S.V., Tarkaev V.V. Classification of Links of Small Complexity in the Thickened Torus. *Proceedings of the Steklov Institute of Mathematics*, 2018, vol. 303, no. 12, pp. 12–24. DOI: 10.1134/S008154381809002X
14. Akimova A.A., Matveev S.V., Tarkaev V.V. Classification of Prime Links in the Thickened Torus Having Crossing Number 5. *Journal of Knot Theory and Its Ramifications*, 2020, vol. 29, no. 3, article ID: 2050012, 27 p. DOI: 10.1142/S0218216520500121
15. Akimova A.A. Tabulation of Prime Links in the Thickened Surface of Genus 2 Having Diagrams with at Most 4 Crossings. *Journal of Computational and Engineering Mathematics*, 2020, vol. 7, no. 3, pp. 20–33. DOI: 10.14529/jcem200303
16. Zinn-Justin P., Zuber J.B. Matrix Integrals and the Generation and Counting of Virtual Tangles and Links. *Journal of Knot Theory and Its Ramifications*, 2004, vol. 13, no. 3, pp. 325–355. DOI: 10.1142/S0218216504003172
17. Zinn-Justin P. *Alternating Virtual Link Database.* Available at: https://www.lpthe.jussieu.fr/pzinn/virtlinks/ (accessed on July 25, 2020).
18. Akimova A.A. Tabulation of Prime Projections of Links in the Thickened Surface of Genus 2 with no More Than 4 Crossings. *Bulletin of the South Ural State University. Series: Mathematics. Mechanics. Physics*, 2020, vol. 12, no. 3, pp. 5–14. DOI: 10.14529/mmph200301
19. Akimova A.A. Classification of Prime Projections of Knots in the Thickened Torus of Genus 2 with at Most 4 Crossings. *Bulletin of the South Ural State University. Series: Mathematics. Mechanics. Physics*, 2020, vol. 12, no. 1, pp. 5–13. DOI: 10.14529/jcem200103
20. Matveev S.V. Prime Decompositions of Knots in $T \times I$. *Topology and its Applications*, 2011, vol. 159, no. 7, pp. 1820–1824.
21. Kauffman L.H. State Models and the Jones Polynomial. *Topology*, 1987, vol. 26, no. 3, pp. 395–407.
22. Jones V.F.R. A Polynomial Invariant for Knots via von Neumann Algebra. *Bulletin of the American Mathematical Society*, 1985, no. 12, pp. 103–111. DOI: 10.1090/s0273-0979-1985-15304-2

23. Tarkaev V.V. *Recognizer of 3D Manifolds.* Available at: http://www.matlas.math.csu.ru.V.F.R
24. Akimova A.A. Generalizations of the Kauffman Polynomial for Knots in the Thickened Surface of Genus 2.*Chelyabinsk Physical and Mathematical Journal*, 2020, vol. 5, no. 3, pp. 352–362
25. Dye H.A., Kauffman L.H. Minimal Surface Representations of Virtual Knots and Links. *Algebraic and Geometric Topology*, 2005, vol. 5, pp. 509–535.
26. Kauffman L.H., Radford D.E. *Bi-Oriented Quantum Algebras, and a Generalized Alexander Polynomial for Virtual Links.* Available at: arXiv:math/0112280
27. Culler M., Dunfield N.M., Goerner M., Weeks J.R. *SnapPy, a Computer Program for Studying the Geometry and Topology of 3-Manifolds.* Available at: http://www.math.uic.edu/t3m/SnapPy

Received March 18, 2022

УДК 515.162 **DOI: 10.14529/mmp220301**

СИСТЕМНЫЙ АНАЛИЗ КЛАССИФИКАЦИИ ПРИМАРНЫХ УЗЛОВ И ЗАЦЕПЛЕНИЙ В УТОЛЩЕННЫХ ПОВЕРХНОСТЯХ РОДА 1 И 2

А.А. Акимова, Южно-Уральский государственный университет, г. Челябинск, Российская Федерация

В данной работе представлен системный анализ подходов к классификации примарных узлов и зацеплений в утолщенных поверхностях рода 1 и 2, полученной автором совместно с С.В. Матвеевым и В.В. Таркаевым в 2012 – 2020 гг. Алгоритм классификации формирует структуру настоящей статьи. Результаты классификации рассматриваются в разрезе системного анализа основных идей ключевых шагов алгоритма. Во-первых, мы строим примарные проекции. Для этого мы определяем понятие примарной проекции зацепления, перечисляем графы специального вида, чье вложение в поверхность может быть примарной проекцией, перечисляем проекции на поверхности и показываем, что все полученные проекции примарны и не эквивалентны, используя ряд инвариантов проекций. Во-вторых, мы строим примарные зацепления. Для этого мы определяем понятие примарного зацепления, строим предварительное множество диаграмм, используем инварианты зацеплений, чтобы сформировать классы эквивалентностей зацеплений и показать, что полученные диаграммы не эквивалентны, и доказываем примарность полученных зацеплений. При этом, на каждом этапе используемые методы и вводимые понятия характеризуются в разрезе двух случаев (род 1 и 2), выделяются как общие, так и характерные только для одного из рассматриваемых случаев свойства. Интерес представляют сводные таблицы, в которых классифицированные проекции систематизированы по свойствам: порождающий граф, род, число компонент и перекрестков, наличие или отсутствие двуугольной грани, что облегчает дальнейшую работу с предлагаемой классификацией проекций и зацеплений.

Ключевые слова: примарная проекция; узел; зацепление; утолщенный тор; утолщенная поверхность рода 2; обобщенный скобочный полином Кауфмана; скелет скобки Кауфмана; табулирование; классификация.

Алена Андреевна Акимова, кандидат физико-математических наук, доцент кафедры математического и компьютерного моделирования; доцент кафедры уравнений математической физики, Южно-Уральский государственный университет (г. Челябинск, Российская Федерация), akimovaaa@susu.ru.

Поступила в редакцию 18 марта 2022 г.